Nanosecond laser-induced breakdown in pure and Yb^{3+} doped fused silica

Arlee V. Smith, Binh Do
Laser, Remote Sensing, Plasma and Complex System Science Department
Sandia National Laboratories, Albuquerque, New Mexico

Mikko Soderlund
Liekki Corporation
Lohja, Finland

The objective of this work is to understand catastrophic optical damage in nanosecond pulsed fiber amplifiers. We used a pulsed, single longitudinal mode, TEM$_{00}$ laser at 1.064 μm, with 7.5-nsec pulse duration, focused to a 7.45-μm-radius spot inside a fused silica window, to measure the single shot optical breakdown threshold irradiances of 4.7E11 and 6.4E11 W/cm^2 respectively for pure fused silica, and for a 1% Yb^{3+} doped fused silica preform of Liekki's Yb1200 fiber. These irradiances have been corrected for self focusing which reduced the area of the focal spot by 10% relative to its low field value. Pulse to pulse variations in the damage irradiance in pure silica was <2%. The damage induction time appears to be much less than 1 ns.

We found the damage morphology was reproducible from pulse to pulse. To facilitate our morphology study we developed a technique for locating the position of the focal waist based on the third harmonic signal generated at the air-fused silica interface. This gives a precise location of the focal position (± 10 μm) which is important in interpreting the damage structure. The surface third harmonic method was also used to determine the diameter of the focal waist.

Earlier reports have claimed the damage irradiance depends strongly on the size of the focal waist. We varied the waist size to look for evidence of this effect, but to date we have found none. We have also studied the temporal structure of the broadband light emitted upon optical breakdown. We find it consists of two pulses, a short one of 16 ns duration, and a long one of several hundred ns. The brightness, spectra, and time profiles of the white light provide clues to the nature of the material modification.

I. Introduction:

Laser induced breakdown leading to optical damage in optically transparent material such as fused silica has been studied by many researchers since the invention of the laser more than four decades ago. It has been important to the development and application of high power lasers because laser induced damage threshold is the ultimate limit to system performance in many cases. Despite this long history we find the literature on nanosecond damage of fused silica is too confusing to use as basis for fiber amplifier design, in part because the reported values of damage threshold irradiance/fluence vary over orders of magnitude. For example, in 1980, Soileau and Bass [1] reported a damage threshold irradiance for fused silica of 605 GW/cm^2 for a pulse duration of 31 ns and a beam radius (I/e^2) of 6.15 μm. More recently, L. Gallais *et al.* [2] reported a damage threshold irradiance for fused silica of 22 ± 5 GW/cm^2 for a pulse duration of 7 ns, and a beam radius (I/e^2) of 6 μm. To determine the ultimate operating limits of fiber amplifiers, we need reliable measurements of the damage threshold and a better understanding of the optical breakdown process. We also need to measure the optical damage threshold of Yb^{3+}-doped fused silica. Additionally, we need to determine whether the optical breakdown threshold is defined by irradiance or fluence.

In order to perform reliable, precise, and reproducible optical breakdown threshold measurements, we must address a number of issues related to the physics of the process. These critical issues, each of which will be addressed in this paper, are:
1. Time and spatial profiles of laser pulses.
2. Detection of optical breakdown.
3. Location and the size of the laser focus.
4. Self focusing.
5. Stimulated Brillouin Scattering (SBS).

After we address each of these issues, we will present our determination of the bulk optical breakdown damage threshold, our study of the damage mechanism and morphology, and our results on the existence of a focal size effect and the influence of Yb^{3+} doping in fused silica.

II. Experimental set-up and technique.
1. Experimental set-up.

Figure 1 shows the experimental apparatus we used for the optical damage measurements. The laser was a flashlamp-pumped, Q-switched, Nd:YAG laser modified to produce a nearly Gaussian spatial beam. The laser was injection seeded to ensure single-longitudinal-mode (smooth pulse) operation. We varied the laser pulse energy delivered to the test sample using a variable attenuator consisting of a half-wave plate and a high-energy cube polarizer. A spatial filter comprising a 200-μm-diameter diamond wire die and an adjustable iris was used to make a near TEM_{00} mode. The beam was focused into the sample by either a 1", 1.5", or 2" focal length best-form lens, depending on the focal spot size desired. The sample was mounted on a motorized 3-dimensional translation stage to enable precise positioning with respect to the focus. We also used two fast phototubes (Hamamatsu R1193U-51) to record the incident and the transmitted pulses, and a photomultiplier (Hamamatsu, R406) to record the broadband light emitted from the breakdown region. A 500 MHz digital oscilloscope recorded the photodetector outputs. Finally, a HeNe probe beam, aligned collinear with the incident pulsed beam, was displayed on a screen positioned beyond the sample to allow visual corroboration of optical damage.
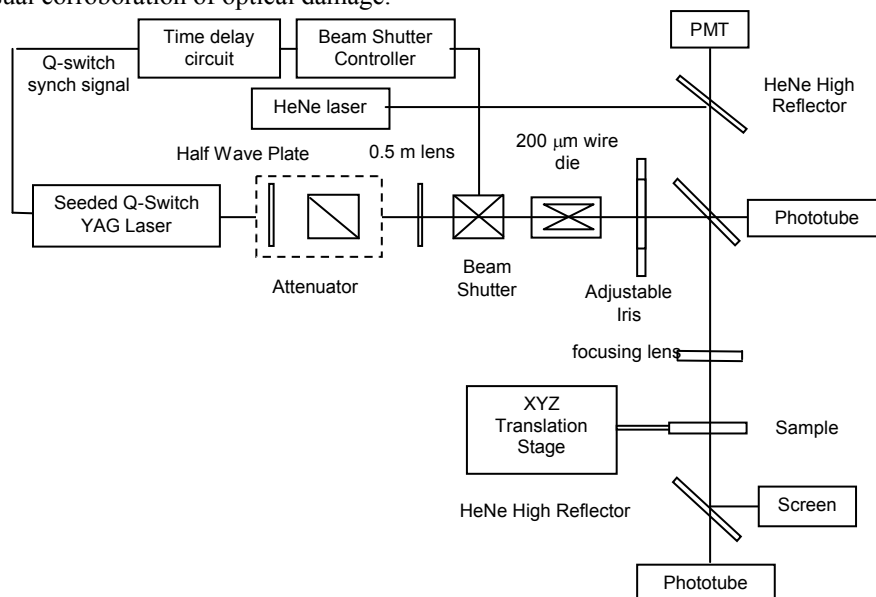

Figure 1: Experimental set-up.

It is worth emphasizing the importance of using a single-longitudinal-mode laser in optical damage measurements. Single-frequency pulses have smooth, well-defined, repeatable temporal shapes that can be reliably measured. In contrast, multi-mode pulses have mode beating and so consist of numerous temporal spikes. As a result, the measurement of the instantaneous laser power at breakdown becomes difficult or impossible. As we will discuss in more detail later, shot-to-shot fluctuation in the peak power of a multi-mode laser are likely responsible for the often reported statistical nature of the damage threshold in fused silica.

For most of our measurements, we used a single laser pulse to damage the sample. The laser pulses were needed on-demand at random times. Although our Nd:YAG laser could run in a truly single-shot mode, the injection seeding control system requires constant feedback at the laser's normal repetition rate of 10 Hz to servo-lock the Q-switched laser cavity length to resonance with the cw seed laser frequency and ensure reliable single-frequency output. In the laser's normal single-shot mode, the laser cavity length is not locked to the seed laser and seeding is unreliable. To avoid this problem, we operated the laser at 10 Hz so that it was reliably injection seeded, and used an electro-mechanical shutter, external to the laser, plus a synchronizing circuit, to extract one or multiple pulses, as needed. This shutter, which can handle the full energy of the laser, is synchronized with the 10-Hz laser operation to open 40 ms before the first desired pulse and to close 40 ms after the last pulse. With this shutter, we can extract any number of laser pulses at any time and be confident that the pulses are single longitudinal mode.

2. Time and spatial profiles of laser pulses.

In order to calculate the optical damage threshold, it is crucial to precisely measure both the spatial and temporal profiles of the laser pulses. As just discussed, our laser produced single-longitudinal-mode pulses with smooth temporal profiles. A typical pulsed waveform is shown in figure 2. The pulse width was 7.5 ns FWHM. Both the pulse shape and the pulse energy were reproducible, with approximately one percent variation in pulse energy from shot to shot.

Figure 2 Temporal shape of the laser pulse. The pulse width is 7.5 ns FWHM.

When we unseed our laser, it runs multimode. The gain bandwidth of Nd:YAG is about 30 GHz, and the free spectral range of our laser is 250 MHz. If we assume that there are 8 equally spaced modes under the gain curve, with amplitudes that obey a Gaussian distribution and phases that are random, the modes interfere with each other to create an output pulse consisting of a series of power spikes, as shown in figure 3. The width of each spike is approximately 15 ps, and the power of the highest spikes can be 4 or more times greater than the maximum power of the seeded pulse of the same energy (yellow curve).
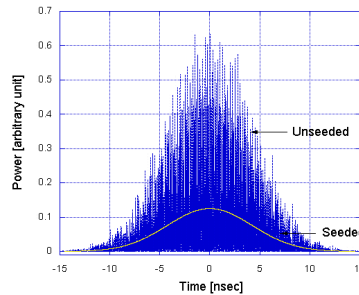

Figure 3: The simulated temporal profile of unseeded and seeded laser pulses of the same energy.

In order for the laser beam to focus predictably its spatial profile should be very close to TEM_{00}. Figure 4 shows the spatial profile of our beam after the focusing lens, just before it entered the sample. This profile was taken by a Coherent Laser Cam HR beam profiling system. The beam profile is well fitted by a Gaussian.
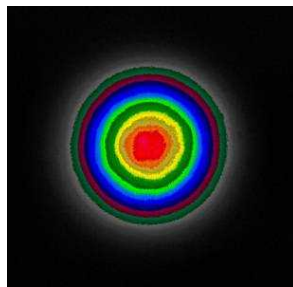

Figure 4: Spatial profile of the laser beam before entering the sample.

3. Detection of optical breakdown.

In the damage process the laser light excites electrons into the conduction band by three processes: tunneling ionization, multiphoton ionization, and impact ionization. When the free electron density reaches a critical density the laser light is strongly absorbed or reflected. This happens when the plasma frequency is equal to the laser frequency

$$\omega_{laser}^2 = \omega_{plasma}^2 = \frac{e^2 n}{m \varepsilon \varepsilon_0},\tag{1}$$

where e is the electron charge, n is the free electron density, m is the electron mass, ε is the relative permittivity of the medium and ε_0 is the free space permittivity. For our 1.064 μm laser, the critical density in fused silica is 2E21/cm^3.

When the optical breakdown begins, the following physical processes occur simultaneously [3]:

a. The generation of a high-density plasma at the focal region that appears as a bright white spot. We detect the white light emitted by this plasma as the primary indicator of optical breakdown.

b. A dramatic decrease in the transmitted laser power as the incident laser pulse is absorbed, reflected and scattered by the dense breakdown plasma in the focal region.

c. A rapid decrease in the transmitted power of the HeNe laser probe beam.

4. Location and the size of the laser focus.

In addition to measuring the breakdown irradiance, we also wish to study the morphology of the breakdown induced damage. These two tasks can be done precisely only if we know the exact location and dimension of the focal spot inside the sample. We found we could measure these two quantities conveniently and precisely by measuring the third-harmonic signal generated by the air-solid interface on the input side of the sample. This third-harmonic signal is due to the broken symmetry of the air-solid interface [4]. The advantages of using the surface third-harmonic method are that it is non-destructive, the uncertainty in locating the surface of the sample is small, at < 10 μm for a 1" focal length lens, and it is much faster than scanning a knife edge. The surface third harmonic pulse energy is proportional to

$$Energy^{(3\omega)} \sim \int_0^\infty \int_0^{2\pi} I_w^3 \exp\left(-6*\frac{r^2}{w^2}\right) r d\theta dr$$

$$= \frac{C}{w^4} = \frac{C}{\left(z_R^2 + [z - z_0]^2\right)^2}.\tag{2}$$

Where w is the beam radius on the surface of the sample, and C is a proportionality constant. Figure 5 shows a typical measurement of the third harmonic signal as a function of the nominal location of the sample input face.
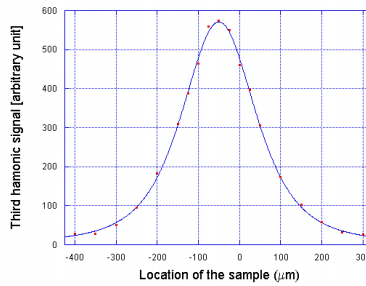

Figure 5: Measured surface third-harmonic signal as the location of the sample was varied.

The surface third-harmonic signal was maximum when the beam waist coincided with the sample surface. We use the width of the third-harmonic signal to determine the focal waist size. We fit the third harmonic signal using a least square fit to eq.(2) with variable z_R, and find the best fit Rayleigh range is z_R = 164 μm in air. This implies a waist size of 7.45 μm for the 1" focal length lens. Our data points fit very well to the curve C/w^4, which was a good indicator that the spatial mode was close to TEM$_{00}$. As a check, we also measured the size of the focal spot using a knife edge and found a value <2% larger than that deduced from the third-harmonic.

6. Self focusing.

The location and size of the focal spot were measured by the third-harmonic method under low irradiance conditions. The optical breakdown threshold irradiance is much higher. The high-intensity beams used for damage testing experience some degree of self focusing due to the nonlinear index of refraction, and, as a result, the focal spot size is reduced. This reduction in spot size must be accounted for in deriving an accurate damage threshold. The refractive index of fused silica is given by

$$n = n_0 + n_2 I. \tag{3}$$

Where n_0, n_2, and I are the linear refractive index, nonlinear refractive index, and the irradiance of the laser beam, respectively. The increase in n with increasing irradiance effectively creates a lens that focuses the beam. Figure 6 shows a Gaussian laser beam focused in fused silica under low field (solid line) and high field (dash line) condition. Under high field conditions, self focusing moves the focus slightly downstream and decreases the waist size, increasing the maximum on-axis irradiance.
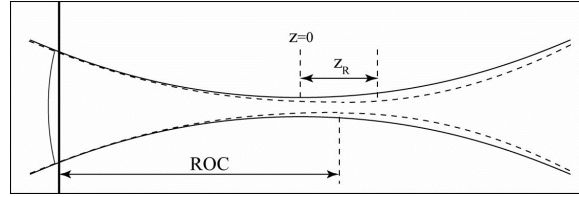

Figure 6: Self focusing moves the focus downstream and increases the maximum irradiance.

The increase of maximum irradiance is a function of the laser power and the depth of focus in the sample. For a low power focal location of z_0 beyond the input surface, the on-axis irradiance at higher power is increased by the amount indicated in Figure 7.
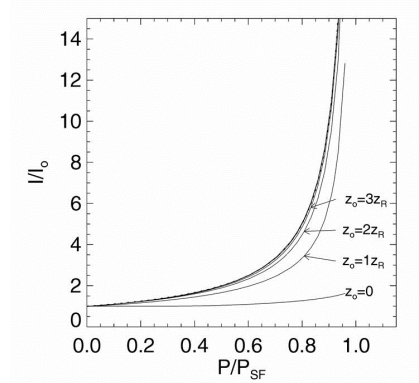

Figure 7: Irradiance enhancement for different depths of focus.

For example, when the low power focus lies 4 or more Rayleigh ranges inside the sample, the irradiance correction factor follows the formula

$$\frac{I_{corr}}{I_0} = \frac{1}{1 - P/P_{sf}} \tag{4}$$

where

$$P_{sf} = \frac{3.73\lambda^2}{8\pi n n_2} \tag{5}$$

Note that the nonlinear refractive index n_2 is different for linearly and circularly polarized light. For linearly polarized light, $P_{sf}(lin) = 4.29$ MW, and for circularly polarized light $P_{sf}(cir) = 5.89$ MW.

7. Stimulated Brillouin Scattering (SBS).

Stimulated Brillouin scattering (SBS) is another nonlinear optical effect that, if present, can taint the results of optical damage experiments. When the SBS process turns on, a large fraction of the laser power is reflected. Because the SBS-reflected beam is nearly a phase conjugate of the pump beam, it interferes with the incident beam to form a moving interference pattern which has significantly higher peak intensity

than the incident pump beam alone. If SBS exists, the apparent breakdown threshold may be incorrect. We can estimate the SBS threshold for a focused Gaussian beam as follows:

$$\text{Gain}_{SBS} = g_0 \, I_0 \, z_R$$

$$= g_0 \, \frac{2P}{\pi w_0^2} \, \frac{\pi w_0^2}{\lambda} = 2g_0 \, \frac{P}{\lambda} \qquad (6)$$

Where g_0 is the SBS gain factor, which is a function of the material, and λ is the laser wavelength. Note that the gain is independent of the strength of focus, or z_R. The threshold for SBS corresponds to a gain of approximately 30. Using Eq. (6) we estimate the power at SBS threshold for 1.064 μm, CW light is 0.3 MW. The SBS build up time is 30 ns, so for a 10 ns, the SBS threshold is roughly estimated to be 0.9 MW.

Experimentally, we found the SBS threshold in D1 fused silica for linearly or circularly polarized light to be 0.86 MW. Figure 8 shows a signature of SBS. The incident and transmitted pulses are shown. The depletion seen late in the transmitted pulse is attributed to SBS reflection. The trailing blip at 50 ns is an SBS reflection. The reflected pulse propagated back into the laser, was amplified and returned to the sample with a 50 ns delay.
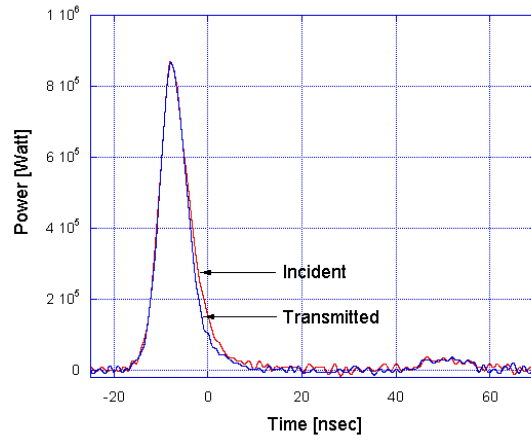

Figure 8: Incident and transmitted waveforms of linearly polarized light at the power slightly above the SBS threshold. w_0=17μm, t_0(FWHM)=7.5ns.

Figure 9 shows the operating regimes, in terms of intensity and spot size, where SBS is expected to be significant for two different pulse lengths: 7.5 ns and 30 ns. We were careful to design our damage experiments to avoid operating in the SBS regime. Also, during the experiments, we monitored the laser waveforms for evidence of a back-reflected SBS pulse (as shown in Figure 8).
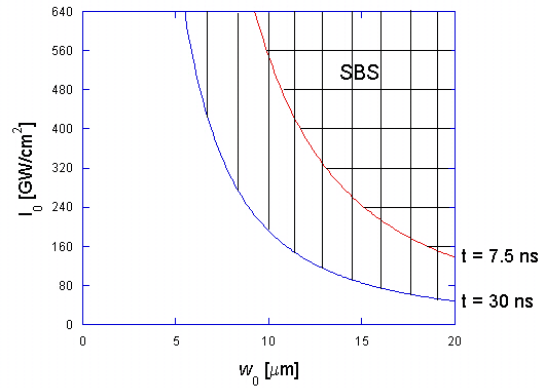

Figure 9: Regimes where SBS is expected to exist are shown as hatched areas for two laser pulse durations: 7.5 ns and 30 ns.

6

III. Experimental results and discussion.

1. Laser induced damage thresholds in fused silica for seeded and unseeded lasers.

This section describes the test procedure and results of optical damage testing on fused silica. The measurements were made using a 1" focal length, best-form lens which focused the beam to 7.45 μm $1/e^2$ radius beam (z_R= 238 μm in fused silica). We first positioned the waist on the surface of the sample using the surface third-harmonic technique described earlier; then moved the focal spot 9.57 mm behind the surface to avoid damaging the front surface. We shot single laser pulses at a fixed transverse (x,y) location and gradually increased the energy until breakdown occurred. We defined optical breakdown as the observation of broadband light emitted from the focal region as monitored by the photomultiplier.

An important observation from this work is that when an injection-seeded pulse was used, the damage threshold was deterministic, not statistical as has often been reported. The difference in pulse energy between 100% damage probability and zero damage probability was less than 2.0%. In fact, for test energies slightly below the damage threshold, the laser could be fired thousands of shots at the same location without evidence of breakdown or optical damage. Yet damage occurred on the first shot when the pulse energy was increased a few percent. The error limit in the damage threshold is the shot-to-shot energy fluctuation of the laser which was approximately 1%. Using the seeded laser, the measured damage threshold was independent of location in the sample, and was the same for different grades of fused silica (Corning grades A0, B0, B1, D0, D1, D3, D5).

For comparison, we also used multimode, unseeded pulses to find the damage threshold. Because of the significant pulse to pulse variation in the unseeded pulses, we fired 3000 shots at each test location for a fixed pulse energy. If we observed damage during those 3000 shots it was counted as damaged, otherwise it was counted as undamaged. This process repeated at ten locations to determine a damage probability at each pulse energy. The transition energy between 0% and 100% probability for the unseeded laser was about 15%. The laser induced damage thresholds in fused silica for seeded and unseeded lasers were shown in figure 10. The optical breakdown induced by a seeded laser was deterministic, or extremely sharp. The data shows the average damage threshold irradiance of unseeded laser beam was about four times smaller than that of the seeded laser beam. This ratio is comparable to the ratio of the power of the highest spike of the unseeded pulse to the maximum power of the seeded pulse of the same energy (fig. 3). This strongly suggests it is irradiance rather than fluence that is the deciding factor for optical breakdown. Further, it suggests that damage is initiated on a 30 ps or shorter time scale. Apparently when using an unseeded laser to measure the optical breakdown threshold of fused silica, we are actually measuring the statistical property of the peak power of the unseeded pulses. Similar results were reported by Glebov [5].
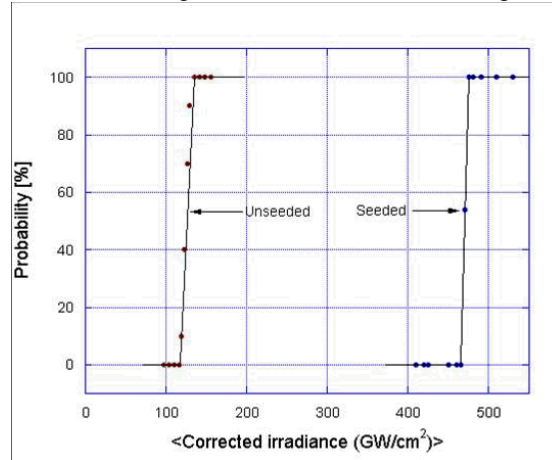

Figure 10: Statistical and deterministic behaviors of optical breakdowns induced by an unseeded laser and a seeded laser.

From an analysis of oscilloscope traces of the incident and transmitted pulses, using the measured pulse energy of the incident pulses for calibration, the damage threshold power of A0 fused silica was 374.2 ± 4.0 kW for linearly polarized light, and 387.7 ± 6.2 kW for circularly polarized light at 1.064 μm. The damage threshold powers were different for these two polarizations because the self focusing effect was different for them. Using the self focusing correction formula

$$\mathrm{I}_{corr} = \frac{\mathrm{I}_0}{1 - \mathrm{P}/\mathrm{P}_{sf}}$$

7

$$, \qquad\qquad (7)$$

where the uncorrected irradiance was defined as

$$I_0 = \frac{2P}{\pi w_0^2} \quad , \qquad\qquad (8)$$

the corrected damage threshold irradiance for linearly polarized light was 470.7 ± 5.0 GW/cm^2, and for circularly polarized light is was 476.4 ± 7.6 GW/cm^2.

By inspecting the waveforms of incident and transmitted pulses whose energy was above the damage threshold pulse energy, we can measure the laser power at the start of the optical breakdown. The waveforms of linearly polarized transmitted pulses at different incident pulse energies are shown in figure 11.
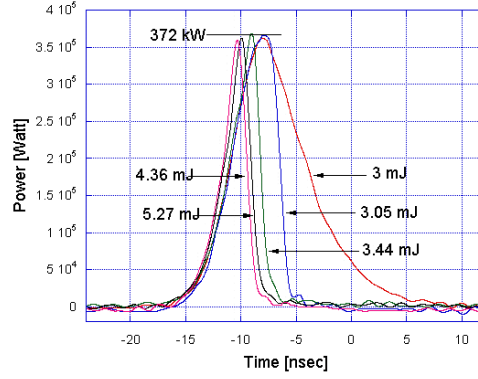

Figure 11: Transmitted waveforms below and above optical breakdown threshold, $w_0 = 7.45$ mm, t_0 (FWHM) = 7.5 ns.

When the incident pulse energy was slightly below the damage threshold (3.0 mJ), the pulse was transmitted through the sample undisrupted, and the sample was undamaged even after 1000 laser pulses. When we increased the incident pulse energy from 3.0 mJ to 3.05 mJ, damage occurred on every shot. We further increased the incident pulse energy incrementally to 5.27 mJ. Figure 11 shows the transmitted pulses. They clearly indicate that breakdown always occurs at nearly constant of 372 kW, indicating breakdown depends only on irradiance and not on fluence for nanosecond pulses.

2. Damage mechanism and morphology.
2a. Broadband light emitted from the optical breakdown in fused silica.
The most reliable indicator of damage is the broadband light emitted from the focal region. The temporal profile of the broadband light is different for different materials, but for bulk damage in fused silica the shape is that shown in Figure 12.
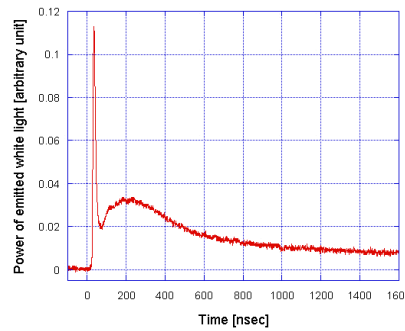

Figure 12: Broadband light emitted from optical breakdown in fused silica.

The broadband light consists of two pulses, a short, 16 ns (FWHM) pulse and a long, several hundred ns pulse. The start of the short pulse coincides with the cutoff of the transmitted pulse. Our speculation about

8

the origin of the broadband light is as follows: At the beginning of optical breakdown, the plasma strongly absorbs the light pulse and generates a large number of free electrons. Subsequently, these free electrons recombine with the positive ions, with radiative recombinations producing the short pulse. Nonradiative recombinations, such as phonon assisted processes, heat the silica matrix in the plasma region and this radiates as a black body with a longer pulse. The broadband light was studied by Carr et al. [6], who found its spectrum matched that of a black body with temperature approximately 7000 K.

2b. Damage morphology.

We studied damage morphologies in the bulk of fused silica using phase contrast microscopy. Figure 13 showes a side view of four optical damage locations created by single longitudinal mode pulses with energies slightly above the damage threshold.
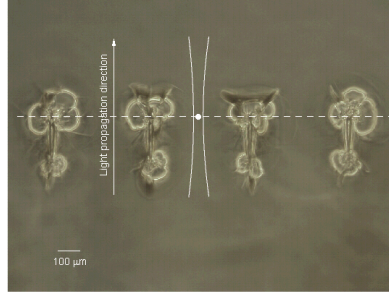

Figure 13: Optical damage locations in fused silica viewed along the propagating direction of the pump beam. The pump pulse energy was slightly above the damage threshold.

The dashed line in the figure indicates the location of the foci. The size of the white dot gives an indication of the uncertainty (±10 μm) in the location of the focal spots, and the two curved lines give an indication of the focal length, or Rayleigh range. They span two Rayleigh ranges, one on either side of the focus. We speculate that damage initiates right at the focus where the light intensity is highest. After breakdown starts and a plasma is formed, the incoming light is absorbed on the upstream edge of the plasma and burns the damage tail or tube as the plasma expands upstream reaching the point where beam expansion weakens the irradiance until it falls below that needed to sustain the plasma. The interesting point was the optical damages were reproducible and always lie in the region between the focus and a point one Rayleigh range upstream from the focus.

3. Focal size effect.

We measured damage threshold irradiances for focal radii of 7.45, 8.18, 12.7 and 17 μm. Thresholds at the 7.45 and 8.18 μm were well below the SBS threshold, and they were nearly identical at 470.7 ± 5.0 and 470.9 ± 4.3 GW/cm^2 for linearly polarized light, and 476.4 ± 7.6 and 479.2 ± 3.2 GW/cm^2 for circularly polarized light. However, for radii of 12.7 and 17 μm, the damage threshold powers exceeded the SBS threshold power. Optical breakdown was assisted by SBS and the damage threshold irradiances were slightly smaller than those at 7.45 and 8.18 μm, as shown in Figure 14.
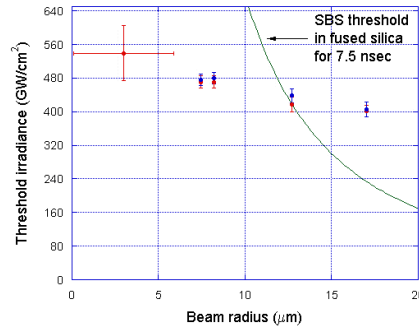
Figure 14: Damage threshold irradiances at different beam radii, the left most and the lower data points for linearly polarized light, and the upper data points for circularly polarized light.

The leftmost datum in figure 14 comes from a measurement that used a 100 mm radius of curvature mirror to retroflect the transmitted laser beam back into the sample. The reflected beam interfered with the incident beam to generate high irradiance anti-nodes spaced by half a wavelength. The idea is that if there is a strong size dependence this fine spatial structure might result in different damage thresholds than a unidirectional beam. We found the threshold pulse energy was a little less than one third of that for unidirectional beam with waists of 7.45 and 8.18 μm. The vertical error bar of this data point is quite large because precise alignment of the retroreflection to overlap the incoming beam is delicate. The horizontal error bar is large because the appropriate focal size is not well defined. We conclude from the results of Figure 14 that the damage threshold is reduced by the SBS, but beyond that there appears to be little influence of focal size on the damage threshold.

4. Influence of Yb^{3+} doping on the damage threshold in fused silica.

We measured the damage threshold irradiance of the Yb doped fiber perform by two methods. For both, the pulse duration is 8.35 ns, and the focal radius was 8.18 μm.

a. In the first method, we selected a transverse location and, starting with an initial pulse energy well below the damage threshold of pure fused silica, we gradually increased the pulse energy by 0.050 mJ per shot until we induced damage.

b. In the second method we fixed the pulse energy 5% above the damage threshold found by method (a), and shot a single pulse at each transverse location in the core of the fiber preform. We deduced the breakdown power from the incident and transmitted pulse waveforms.

The difference between the threshold irradiances measured by these two methods differed by less than 3%, $I_{corr-lin}$ = 640 ± 19 GW/cm^2. Thus, the damage threshold of 1% Yb^{3+}-doped silica appears to be 35% higher than that of pure silica. However, we consider the doped silica thresholds preliminary because optical distortion in the preform cores causes uncertainty about the focal conditions and thus of the damage threshold. Further damage threshold measurements will be conducted on perform samples from Liekki and other manufacturers.

IV. Conclusions.

We find the damage threshold irradiance in fused silica is 471 ± 5.0 GW/cm^2 and 476 ± 7.6 GW/cm^2 for linearly and circularly polarized light, respectively. The damage threshold is deterministic, not statistical as has often been reported. We corrected the damage threshold irradiances for self focusing. From our experiments we see that the damage produced by ns pulses occurrs at a precise threshold irradiance, not a threshold fluence. Comparison of thresholds for seeded and unseeded pulses indicates that optical breakdown is initiated on a time scale of 30 ps or less. The damage threshold irradiance is reduced by SBS, and we find no clear evident of a focal size effect. Our preliminary determination of the damage threshold irradiance of 1% Yb^{3+}-doped fiber preform is 640 ± 19 GW/cm^2.

References
1. M. Soileau and M. Bass, IEEE J. Quantum Electron.,**QE-16**,No. 8, 814 (1980).
2. L. Gallais, J. Natoli, C. Amra, Optics Express, **10**, 1465 (2002).
3. N. Bloembergen, IEEE J. Quantum Electron., **QE-10**, No. 3, 375 (1974).
4. T. Tsang, Phys. Rev. A, **52**, 4116 (1995).
5. L. Glebov, Proceeding of SPIE, Vol. 4679, 321 (2002).
6. C. Carr, H. Radousky, A. Rubenchik, M. Feit, and S. Demos, Phys. Rev. Lett., **92**, 087401 (2004).